On the Effective Capacity of RIS-enabled mmWave Networks with Outdated CSI

Syed Waqas Haider Shah*†, *Member, IEEE*, Sai Pavan Deram*, and Joerg Widmer*, *Fellow, IEEE*
*IMDEA Networks Institute, Madrid, Spain
†Information Technology University, Lahore, Pakistan
{syed.waqas, sai.deram, joerg.widmer}@imdea.org

***Abstract*—Reconfigurable intelligent surfaces (RISs) have great potential to improve the coverage of mmWave networks; however, acquiring perfect channel state information (CSI) of a RIS-enabled mmWave network is very costly and should thus be done infrequently. At the same time, finding an optimal RIS configuration when CSI is outdated is challenging. To this end, this work aims to provide practical insights into the tradeoff between the outdatedness of the CSI and the system performance by using the effective capacity as analytical tool. We consider a RIS-enabled mmWave downlink where the base station (BS) operates under statistical quality-of-service (QoS) constraints. We find a closed-form expression for the effective capacity that incorporates the degree of optimism of packet scheduling and correlation strength between instantaneous and outdated CSI. Moreover, our analysis allows us to find optimal values of the signal-to-interference-plus-noise-ratio (SINR) distribution parameter and their impact on the effective capacity in different network scenarios. Simulation results demonstrate that better effective capacity can be achieved with suboptimal RIS configuration when the channel estimates are known to be outdated. It allows us to design system parameters that guarantee better performance while keeping the complexity and cost associated with channel estimation to a minimum.**

***Index Terms*—Reconfigurable intelligent surface, millimeter-wave communication, effective capacity, qulaity-of-service, channel state information**

I. Introduction

Fifth-generation (5G) networks are experiencing an ever-increasing demand for high data rates, extremely low latency, and ultra-reliability from a massive number of connected users. Wireless networks operating at sub-6 GHz frequencies are quickly becoming a bottleneck in the effective rollout of 5G networks as they are unable to fulfill these demands from an exponentially growing number of users due to the scarcity of spectrum resources [1]. In contrast, millimeter wave (mmWave) networks have the capability to overcome these challenges by exploiting the vast and largely unused frequency spectrum ranging from 30 to 300 GHz. Communication at mmWave frequencies promises to provide several benefits, including but not limited to an order of magnitude increase in throughput, latencies of less than 10 ms, and enough bandwidth to provide access to a massive number of users [2]. However, mmWave communication suffers from penetration loss and much higher overall path loss compared to sub-6 GHz communication, and is thus susceptible to blockages caused by objects in the environment. These challenges limit the deployment scope of mmWave networks to comparatively short distances [3].

Recently, the concept of reconfigurable intelligent surfaces (RISs) has emerged, which has the potential to overcome several of the challenges faced by mmWave networks. A RIS is a software-defined metasurface containing a large number of scattering elements (also known as unit cells), which can passively beamform the incident signals towards the intended user(s). The unit cells are passive elements that have the capability to adjust the incident signals' amplitude and phase responses by using a low-cost and low-power RIS controller [4]. This phenomenon allows the RIS to turn an uncontrolled wireless environment into a controlled and reconfigurable one. A RIS can effectively be used for the transmission distance extension of mmWave communication without increasing the energy budget of a network [5].

The performance of a RIS-assisted network critically depends upon the channel estimation, as these estimates are used to configure the RIS elements. As the channel estimate ages, the performance degrades, which can be addressed by estimating the channel more frequently. However, perfect instantaneous channel state information (CSI) is hard to come by, especially for mmWave networks, where the channel conditions change rapidly over time [6, 7]. Also, mmWave networks use large antenna arrays both at the transmitter and receiver to compensate for the higher path loss, which makes the channel estimation even more difficult for RIS-enabled mmWave networks [8]. Moreover, the signaling overhead associated with acquiring perfect CSI is very high for RIS-enabled mmWave networks because the corresponding channel matrices are extremely large due to the presence of an intermediate RIS [9, 10]. Since a RIS itself cannot estimate the channel, the BS (in case of a downlink) performs the estimation for the end-to-end communication channel through feedback links, which results in large delays and higher complexity [11]. Beyond that, with higher user mobility, acquiring perfect channel estimates would entail extremely high signaling overhead and even larger delays, which consequently has the potential to evolve into a bottleneck for channel estimation [12].

These considerations raise several questions on the estimation quality of a RIS-enabled mmWave channel. First and foremost, how often should a RIS-enabled mmWave channel be estimated given different network conditions? How much signaling overhead would that cause, and how it will affect

the overall performance of the network? Intuitively, the higher the quality of estimation, the higher the overhead, and vice versa, which requires finding the right tradeoff to optimize channel capacity [13]. However, to the best of the authors' knowledge, there is no study available that provides practical insights into these string of questions. Second, in the case of outdated CSI (to maintain a manageable signaling overhead), what is the tradeoff between the outdatedness of the CSI and RIS configuration and again, what impact does it have on the network performance? In other words, how optimized should the RIS configuration be for the current CSI that is known to be outdated? Last but not least, given the outdated CSI, how should the system parameters be designed to guarantee good performance while keeping the complexity and cost associated with channel estimation to a minimum? These questions are extremely important, particularly, for mmWave networks because, in these networks, the RIS uses narrow beams to communicate with the user. If the RIS is configured using outdated channel estimates and if the user is mobile, the transmit beam might miss the user entirely, which will cause an outage.

To this end, this work investigates these questions to provide insights into the different tradeoffs. We leverage a link-layer analytical model, effective capacity (EC), for our analysis. When a transmitter operates under certain quality-of-service (QoS) constraints, the EC provides a maximum sustainable constant arrival rate at the transmission queue in the face of a randomly time-varying wireless channel [14]. We find a closed-form expression for the EC of the RIS-enabled mmWave communication network, which provides insights into a tradeoff between the degree of optimism of packet scheduling at the BS and the correlation strength between the instantaneous and outdated CSI, and also investigates their impact on the achievable EC. Our analysis provides an in-depth discussion of the impact of correlation strength on the probability distribution function (PDF) of the received signal-to-interference-plus-noise-ratio (SINR), which can help network service providers with RIS configuration as well as RIS placement in different network conditions.

The rest of the paper is organized as follows. In Section II, we summarize the existing literature related to the topic. Section III provides the system model used for the analysis. In Section IV, we introduce the RIS-enabled mmWave channel and find the PDF of the received SINR. Section V presents the EC analysis. Simulation results with discussions are presented in Section VI, and we draw conclusions in Section VII.

II. Related Works

Most prior works on RIS-assisted wireless networks consider a perfect or a statistical CSI at hand to configure the RIS elements for capacity and coverage enhancement. In [15], a channel capacity optimization scheme was proposed for an indoor RIS-enabled mmWave network. The proposed scheme maximizes the channel capacity by adjusting the RIS elements using a global and a local co-phasing mechanism. In [16], the authors use the statistical CSI to jointly optimize the transmit covariance matrix and the phases of the RIS elements to maximize the ergodic capacity of a RIS-enabled mmWave MIMO channel. The authors in [17] perform the throughput analysis of a RIS-assisted channel by considering both statistical and perfect CSI at the transmitter. When the transmitter sends data without prior knowledge of the CSI, the packet drop ratio increases, and to address that, the authors use retransmission schemes to improve the throughput. Despite the fact that these and other similar works which assume perfect or statistical CSI present notable improvements in achievable capacities and system performance, their practicality in real-time systems is still undecided. The improvements made in these works may be considered an upper bound for the network performance as they do not consider the real-time random behavior of the channels. Although there have been various solid efforts to estimate RIS-enabled mmWave channels ([18–23] and references therein), perfect channel estimation is not only difficult, it is also not practical due to the very large measurement and signaling overhead associated with it [24].

Despite extensive works on RIS-assisted wireless networks, only few studies consider the outdated channel information for capacity analysis and network performance. Some works that do consider outdated CSI do not provide many insights into its impact on the overall performance. In [25], the authors use the outdated CSI to jointly optimize the transmit beamforming and the RIS' reflecting beamforming matrices to enhance the secrecy rate. Although this work investigates the impact of several factors such as transmit power, the number of users, eavesdroppers, and RIS elements on the secrecy capacity of the RIS-assisted network, it does not provide much detail on the impact of outdated CSI. In another work [26], a deep reinforcement learning (DRL)-based secure transmission mechanism for RIS-enabled mmWave unmanned aerial vehicle communication under the assumption of outdated CSI is presented. The authors proposed a maximization problem for the secrecy rate given the secrecy outage probability resulting from an outdated CSI error model. In [27], a DRL-based spectral efficiency enhancement mechanism is given for a RIS-enabled mmWave high-speed railway Network. Through numerical simulations, the authors investigate the impact of outdated CSI coefficients on the spectral efficiency of the network. More recently, in [28], the authors proposed a RIS deployment mechanism in centralized and distributed scenarios given the outdated CSI. They find the ergodic capacity for both the scenarios and highlight the importance of correlation strength between outdated and instantaneous CSI.

Despite considering outdated CSI in their analysis, the above studies do not provide deeper insights into the *impact* of outdated CSI on the performance of a RIS-assisted network. Many questions related to the quality of estimating a RIS-enabled mmWave channel, as well as its impact on the signaling overhead and the practical aspects behind using the outdated CSI instead of instantaneous CSI, are still unanswered in the literature. To this end, this work aims to answer these questions by performing a statistical QoS analysis of a RIS-enabled mmWave network with outdated CSI.

III. System Model

We consider the downlink of a RIS-enabled mmWave communication network[1], as shown in Fig. 1, in which the BS is equipped with N_B antennas to communicate with K single-antenna mobile stations (MSs) with the assistance of a RIS with N_R passive reflecting elements. Each RIS element is capable of independently adjusting its phase shift to reflect the incident signals toward desired users. For the channel, we consider that the direct link between BS and MS is blocked by obstacles and only the reflected/cascaded link (via the RIS) is available for transmission. The transmit antennas at the BS and the RIS elements are placed in a uniform linear array (ULA) and a uniform rectangular array (URA), respectively. To reduce the propagation loss for BS→RIS and RIS→MS links, we assume that the ULA and URA elements can adaptively adjust the weights on each omnidirectional antenna element at the BS and each RIS element, respectively, for beamforming.

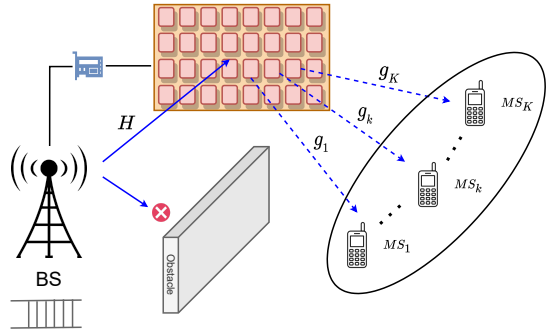

Fig. 1. RIS-enabled mmWave communication network for multiple single-antenna users: solid blue arrows show incident wave and dotted blue arrows represent reflected waves.

Let $N_R = \{1, 2, \ldots, N_R\}$, $N_B = \{1, 2, \ldots, N_B\}$, $K = \{1, 2, \ldots, K\}$ represent the set of RIS elements, transmit antennas at the BS, and the single-antenna MSs, respectively. Let $\mathbf{H} \in \mathbb{C}^{N_R \times N_B}$, $\mathbf{g}_k \in \mathbb{C}^{1 \times N_R}$, $\mathbf{f}_k = \{f_{k,1}, f_{k,2}, \ldots, f_{k,N_B}\}$, and s_k represent the channel coefficients between the BS and the RIS, channel coefficients between the RIS and the k^{th} MS, the transmit precoding vector at the BS, and the transmitted symbol for the k^{th} MS, respectively. We also consider that both channels ($\mathbf{H}$ and $\mathbf{g}_k$) follow Rician fading. Thus, by considering the line of sight (LoS) and non-LoS (NLoS) paths, we can express the channels as

$$\begin{aligned} \mathbf{H} &= \sqrt{\frac{\mathcal{K}_B}{1+\mathcal{K}_B}}\mathbf{H}^{LoS} + \sqrt{\frac{1}{1+\mathcal{K}_B}}\mathbf{H}^{NLoS} \\ \mathbf{g}_k &= \sqrt{\frac{\mathcal{K}_R}{1+\mathcal{K}_R}}\mathbf{g}_k^{LoS} + \sqrt{\frac{1}{1+\mathcal{K}_R}}\mathbf{g}_k^{NLoS}. \end{aligned} \tag{1}$$

[1]Note that we determine the EC of a RIS-enabled mmWave downlink; however, the analysis presented in this work can be easily extended to the uplink by exploiting the duality property of uplink and downlink.

In (1), $\mathcal{K}_B$ and $\mathcal{K}_R$ represent the Rician K-factor. As a result, the received signal at the k^{th} MS can be written as

$$y_k = (\mathbf{g}_k \mathbf{\Omega} \mathbf{H})\mathbf{f}_k s_k + \sum_{i=1, i\neq k}^{K} (\mathbf{g}_k \mathbf{\Omega} \mathbf{H})\mathbf{f}_i s_i + n_k. \tag{2}$$

In (2), $\mathbf{\Omega} \in \mathbb{C}^{N_R \times N_R}$ represents the phase control matrix at the RIS. Note that $\mathbf{\Omega}$ is a diagonal matrix ($\mathbf{\Omega} = \text{diag}[\pi_1, \pi_2, \ldots, \pi_n, \ldots, \pi_{N_R}]$), where $\pi_n = e^{j\theta_n}$ and θ_n is the phase shift introduced by n^{th} RIS element. Here, we assume that the channel between the BS and the RIS ($\mathbf{H}$) can be known perfectly since the locations of the BS and the RIS are generally taken as fixed; hence, optimal values of the transmit beamforming vector ($\mathbf{f}_k$) are known at the BS. However, for the channel between the RIS and the k^{th} MS ($\mathbf{g}_k$), acquiring perfect channel estimates is difficult and costly, due to MS mobility. Therefore, the optimal configuration of the phase control matrix at the RIS ($\mathbf{\Omega}$) is usually not available. To this end, the next section provides an investigation of a RIS-enabled mmWave channel when only outdated channel estimates are available for RIS configuration.

IV. RIS-enabled mmWave Channel with Outdated CSI

In this section, we investigate a RIS-enabled mmWave network with multiple users under the condition that the BS only has access to outdated channel estimates for configuring its elements. We find the PDF and a closed-form expression for the distribution parameter of the SINR at the user, which incorporates the correlation strength between the outdated and instantaneous CSI. This PDF and the expression for the distribution parameter will allow us to perform an EC analysis of the RIS-enabled mmWave channel for different network conditions (presented in Section V). Based on that analysis, we can configure system parameters that guarantee better performance while ensuring the cost and complexity associated with channel estimation remains low.

Perfect channel estimation for the RIS → MS_k link is usually not possible due to acquisition delay and large signaling overhead, which can become even larger with MS mobility (details are given in Sections I and II). Therefore, we consider that only outdated channel estimates for the RIS → MS_k link are available. Let T_{delay} denote the delay between the outdated CSI and the instantaneous CSI. As shown in [25], the relation between the outdated channel vector $\mathbf{g}_k(t)$ and the instantaneous channel vector $\mathbf{g}_k(t + T_{delay})$ can then be written as

$$\mathbf{g}_k = \rho \hat{\mathbf{g}}_k + \bar{\rho}\mathbf{w}_k, \tag{3}$$

where $\mathbf{g}_k = \mathbf{g}_k(t + T_{delay})$, $\hat{\mathbf{g}}_k = \mathbf{g}_k(t)$, $\mathbf{w}_k = \hat{\mathbf{g}}_k(t + T_{delay})$, ρ is the correlation coefficient between the outdated channel estimate $\hat{\mathbf{g}}_k$ and the actual channel $\mathbf{g}_k$, and $\bar{\rho} = \sqrt{1 - \rho^2}$. It is also important to note that $0 \leq \rho \leq 1$, where $\rho = 0$ and $\rho = 1$ represent the perfect CSI and no CSI, respectively. Moreover, ρ can be calculated using $\rho = J_0(2\pi f_D T_{delay})$. Here, f_D is the maximum Doppler shift, with $f_D = f_c v/c$, where f_c is the carrier frequency, v is the velocity with which the MS

is moving, and c is the speed of light. Furthermore, $\mathbf{w}_k = [w_{k,1}, w_{k,2}, \ldots, w_{k,n}, \ldots, w_{k,N_R}]$, where $w_{k,n}$ is independent and identically distributed with $g_{k,n}$ and $\hat{g}_{k,n}$, and it follows a complex Guassian distribution with zero mean and variance $\sigma^2_{\hat{g}_{k,n}}$ (i.e., $w_{k,n} \sim \mathcal{CN}(0, \sigma^2_{\hat{g}_{k,n}})$).

By incorporating the impact of the outdated CSI on $\mathbf{g}_k$ in (2), the received signal under the channel uncertainty model becomes

$$y_k = (\{\rho\hat{\mathbf{g}}_k + \bar{\rho}\mathbf{w}_k\}\mathbf{\Omega}\mathbf{H})\mathbf{f}_k s_k + \sum_{i=1, i\neq k}^{K} (\{\rho\hat{\mathbf{g}}_k + \bar{\rho}\mathbf{w}_k\}\mathbf{\Omega}\mathbf{H})\mathbf{f}_i s_i + n_k, \tag{4}$$

where n_k is the additive complex Gaussian noise (AWGN) with with zero mean and σ_k^2 variance at the k^{th} MS ($n_k \sim \mathcal{CN}(0, \sigma_k^2)$). By separating the desired signal from the outdated CSI noise and the inter-user interference, the expression for the received signal at the k^{th} MS in (4) can be re-written as

$$y_k = \underbrace{\{\rho\hat{\mathbf{g}}_k\mathbf{\Omega}\mathbf{H}\}\mathbf{f}_k s_k}_{\text{desired signal}} + \underbrace{\{\bar{\rho}\mathbf{w}_k\mathbf{\Omega}\mathbf{H}\}\mathbf{f}_k s_k}_{\text{outdated CSI noise}} + \underbrace{\sum_{i=1, i\neq k}^{K} \{\rho\hat{\mathbf{g}}_k\mathbf{\Omega}\mathbf{H}\}\mathbf{f}_i s_i + \underbrace{\sum_{i=1, i\neq k}^{K} \{\bar{\rho}\mathbf{w}_k\mathbf{\Omega}\mathbf{H}\}\mathbf{f}_i s_i}_{\text{outdated CSI noise}} + n_k}_{\text{inter-user interference}}. \tag{5}$$

Next, we need to find the SINR of the received signal, which will allow us to find the EC of the RIS-enabled mmWave channel. By using the expression in (5), the received SINR becomes

$$\gamma_k = \frac{|\rho\hat{\mathbf{g}}_k\mathbf{\Omega}\mathbf{H}\mathbf{f}_k|^2}{\sigma^2_{MM}}. \tag{6}$$

In (6), σ^2_{MM} represents the cumulative noise (outdated plus thermal) and interference (caused by other users present in the network) experienced by the received signal at k^{th} MS, which can be calculated as

$$\sigma^2_{MM} = \mathbb{E}\Bigg[|\bar{\rho}\mathbf{w}_k\mathbf{\Omega}\mathbf{H}\mathbf{f}_k|^2 + |\sum_{i=1, i\neq k}^{K} \rho\hat{\mathbf{g}}_k\mathbf{\Omega}\mathbf{H}\mathbf{f}_i|^2 + |\sum_{i=1, i\neq k}^{K} \bar{\rho}\mathbf{w}_k\mathbf{\Omega}\mathbf{H}\mathbf{f}_i|^2 + |n_k|^2\Bigg]. \tag{7}$$

By separating each term to simplify the calculation, the expression in (7) can be re-written as

$$\sigma^2_{MM} = \bar{\rho}^2\mathbb{E}\big[|\mathbf{w}_k\mathbf{\Omega}\mathbf{H}\mathbf{f}_k|^2\big] + \rho^2\mathbb{E}\big[|\sum_{i=1, i\neq k}^{K} \hat{\mathbf{g}}_k\mathbf{\Omega}\mathbf{H}\mathbf{f}_i|^2\big] + \bar{\rho}^2\mathbb{E}\big[|\sum_{i=1, i\neq k}^{K} \mathbf{w}_k\mathbf{\Omega}\mathbf{H}\mathbf{f}_i|^2\big] + \sigma_k^2, \tag{8}$$

where $\mathbb{E}\big[|n_k|^2\big] = \sigma_k^2$ is the variance of the AWGN. Next, we aim to solve the cumulative noise and interference given in (8), which will consequently help finding the PDF of the received SINR and the closed-form expression for the SINR distribution parameter.

For finding the ensemble mean of the outdated CSI noise, we leverage Appendix B in [28], which solves a SISO model, and extend it for our system model with $\mathbf{H} \in \mathbb{C}^{N_R \times N_B}$ and a transmit beamforming vector $\mathbf{f}_k$. Lemma 1 provides the ensemble mean of the outdated CSI noise.

Lemma 1. $\mathbb{E}\big[|\mathbf{w}_k\mathbf{\Omega}\mathbf{H}\mathbf{f}_k|^2\big] = (1-\alpha^2)\sum_{b=1}^{N_B}|f_{k,b}|^2$. *Where, α is the average value of Rician variable $|\hat{g}_{k,n}(t+T_{delay})|$, which can be found using Appendix A in [29].*

Proof:

$$\mathbb{E}\big[|\mathbf{w}_k\mathbf{\Omega}\mathbf{H}\mathbf{f}_k|^2\big] = \mathbb{E}\Bigg[\Bigg|\sum_{n=1}^{N_R}\sum_{b=1}^{N_B} w_{k,n}h_{n,b}e^{j\theta_n}f_{k,b}\Bigg|^2\Bigg] = \mathbb{E}\Bigg[\Bigg|\sum_{n=1}^{N_R}\sum_{b=1}^{N_B}\sum_{m=1}^{N_R}\sum_{a=1}^{N_B} w_{k,n}h_{n,b}e^{j\theta_n}f_{k,b}w^*_{k,m}h^*_{m,a}e^{-j\theta_m}f_{k,a}\Bigg|\Bigg] \tag{9}$$

$$\mathbb{E}\big[|\mathbf{w}_k\mathbf{\Omega}\mathbf{H}\mathbf{f}_k|^2\big] = \underbrace{\sum_{n=1}^{N_R}\sum_{b=1}^{N_B}\mathbb{E}\Big[|w_{k,n}|^2|h_{n,b}|^2|f_{k,b}|^2\Big]}_{\mathrm{a}_1} + \underbrace{\sum_{n=1}^{N_R}\sum_{b=1}^{N_B}\sum_{m=1,m\neq n}^{N_R}\sum_{a=1,a\neq b}^{N_B}\mathbb{E}\Big[w_{k,n}h_{n,b}w^*_{k,m}h^*_{m,a}f_{k,b}f_{k,a}\Big]e^{j(\theta_x)}}_{\mathrm{a}_2}. \tag{10}$$

Here $\theta_x = \theta_n - \theta_m$. Note that $\mathbf{w}_k$ and $\mathbf{H}$ are independent of each other and $\mathbb{E}[w_{k,n}] = 0$. Therefore, a_2 becomes zero. Moreover, $h_{n,b} \sim \mathcal{CN}(0,1)$ and $\mathbb{E}\big[|w_{k,n}|^2\big] = \sigma^2_{\hat{g}_{k,n}(t+T_{delay})} = 1-\alpha^2$. Thus, (9) becomes

$$\begin{aligned}\mathbb{E}\big[|\mathbf{w}_k\mathbf{\Omega}\mathbf{H}\mathbf{f}_k|^2\big] &= \sum_{n=1}^{N_R}\sum_{b=1}^{N_B}\mathbb{E}\big[|w_{k,n}|^2\big]\mathbb{E}\big[|h_{n,b}|^2\big]|f_{k,b}|^2 \\ &= \sum_{n=1}^{N_R}\sum_{b=1}^{N_B}\sigma^2_{\hat{g}_{k,n}(t+T_{delay})}\big(\sigma^2_{h_{n,b}} + \mathbb{E}\big[|h_{n,b}|\big]^2\big)|f_{k,b}|^2 \\ &= (1-\alpha^2)\sum_{b=1}^{N_B}|f_{k,b}|^2.\end{aligned} \tag{11}$$

■

Next, by following steps similar to those given in Lemma 1, we can also find the ensemble mean of the inter-user interference experienced by the received signal, which becomes

$$\begin{aligned}\mathbb{E}\big[|\sum_{i=1, i\neq k}^{K}\hat{\mathbf{g}}_k\mathbf{\Omega}\mathbf{H}\mathbf{f}_i|^2\big] &= (1-\beta^2)\sum_{b=1}^{N_B}|f_{i,b}|^2 \\ \mathbb{E}\big[|\sum_{i=1, i\neq k}^{K}\mathbf{w}_k\mathbf{\Omega}\mathbf{H}\mathbf{f}_i|^2\big] &= (1-\alpha^2)\sum_{b=1}^{N_B}|f_{i,b}|^2.\end{aligned} \tag{12}$$

Now, for the final expression of the cumulative noise and interference, we substitute the ensemble mean values from (11) and (12) into (8), which gives

$$\sigma^2_{MM} = \bar{\rho}^2(1-\alpha^2)\sum_{b=1}^{N_B}|f_{k,b}|^2 + \rho^2(1-\beta^2)\sum_{i=1, i\neq k}^{K}\sum_{b=1}^{N_B}|f_{i,b}|^2 + \bar{\rho}^2(1-\alpha^2)\sum_{i=1, i\neq k}^{K}\sum_{b=1}^{N_B}|f_{i,b}|^2 + \sigma_k^2. \tag{13}$$

After some simplification steps, the expression in (13) becomes

$$\sigma_{MM}^2 = \bar{\rho}^2(1-\alpha^2)\sum_{i=1}^{K}\sum_{b=1}^{N_B}\left|f_{i,b}\right|^2+\rho^2(1-\beta^2)\sum_{i=1,i\neq k}^{K}\sum_{b=1}^{N_B}\left|f_{i,b}\right|^2+\sigma_k^2. \tag{14}$$

Now, by substituting the expression in (14) into (6), we can find the received SINR at the k^{th} MS (γ_k). Since we have the final expression for the received SINR, we can find its PDF. Moreover, we also need to find the expression for the distribution parameter of the PDF, which will define the statistical dispersion of the PDF. To this end, Lemma 2 provides the PDF and the expression for the distribution parameter for the received SINR γ_k given in (6).

Lemma 2. *The received SINR of the RIS-assisted multi-user MISO network at the k^{th} MS during time slot l follows an exponential distribution: $\gamma_k(l) \sim \exp(\xi)$, where ξ is the exponential parameter and can be calculated using the following expression*

$$\xi = \frac{\left\{\Upsilon_1 + \Upsilon_2 + \sigma_k^2\right\}^2}{2N_R^2\left(\sum_{n=1}^{N_R}\sum_{b=1}^{N_B} e^{j2\theta_n}|f_{k,b}|^2\right)^2}.$$

where $\Upsilon_1 = \bar{\rho}^2(1-\alpha^2)\sum_{i=1}^{K}\sum_{b=1}^{N_B}\left|f_{i,b}\right|^2$ *and* $\Upsilon_2 = \rho^2(1-\beta^2)\sum_{i=1,i\neq k}^{K}\sum_{b=1}^{N_B}\left|f_{i,b}\right|^2$.

Proof: In order to compute the distribution of the received SINR of the RIS-assisted multi-user MISO network at the k^{th} MS, we start by assuming that both the RIS and the BS have two reflecting elements and transmitting antennas, respectively ($N_R = N_B = 2$). It allows us to write

$$\begin{aligned}\hat{\mathbf{g}}_k\mathbf{\Omega}\mathbf{H}\mathbf{f}_k = \hat{g}_{k,1}e^{j\theta_1}(f_{k,1}h_{1,1} + f_{k,2}h_{1,2})\\ + \hat{g}_{k,2}e^{j\theta_2}(f_{k,1}h_{2,1}, +f_{k,2}h_{2,2}).\end{aligned} \tag{15}$$

Let $\Psi_1 = \hat{g}_{k,1}e^{j\theta_1}(f_{k,1}h_{1,1} + f_{k,2}h_{1,2})$ and $\Psi_2 = \hat{g}_{k,2}e^{j\theta_2}(f_{k,1}h_{2,1} + f_{k,2}h_{2,2})$. Here, we remind again that $\hat{g}_{k,n} \sim \mathcal{CN}(0,1)$ and $h_{n,b} \sim \mathcal{CN}(0,1)$ for $n \in \{1,2\}$ and $b \in \{1,2\}$. Then, one can verify that $\Psi_1 \sim \mathcal{CN}\big(0, e^{j2\theta_1}(|f_{k,1}|^2 + |f_{k,2}|^2)\big)$ and $\Psi_2 \sim \mathcal{CN}\big(0, e^{j2\theta_2}(|f_{k,1}|^2 + |f_{k,2}|^2)\big)$. We note that $\hat{\mathbf{g}}_k\mathbf{\Omega}\mathbf{H}\mathbf{f}_k$ is the sum of two independent and identically distributed complex Gaussian random variables when $N_R = N_B = 2$. Thus, in general, we can write, $\hat{\mathbf{g}}_k\mathbf{\Omega}\mathbf{H}\mathbf{f}_k = \sum_{n=1}^{N_R}\mathcal{Z}_n$, where $\mathcal{Z}_n \sim \mathcal{CN}(0, \sum_{n=1}^{N_R}\sum_{b=1}^{N_B} e^{j2\theta_n}|f_{k,b}|^2)$. The term $\hat{\mathbf{g}}_k\mathbf{\Omega}\mathbf{H}\mathbf{f}_k$ is thus the sum of N_R independent and identically distributed complex Gaussian random variables. In case N_R is reasonably large, we can invoke the Central Limit Theorem to get the following approximation: $\hat{\mathbf{g}}_k\mathbf{\Omega}\mathbf{H}\mathbf{f}_k \sim \mathcal{CN}\left(0, N_R\sum_{n=1}^{N_R}\sum_{b=1}^{N_B} e^{j2\theta_n}|f_{k,b}|^2\right)$. This implies that $|\hat{\mathbf{g}}_k\mathbf{\Omega}\mathbf{H}\mathbf{f}_k|$ follows the Rayleigh distribution, $|\hat{\mathbf{g}}_k\mathbf{\Omega}\mathbf{H}\mathbf{f}_k| \sim Rayleigh\left(N_R\sum_{n=1}^{N_R}\sum_{b=1}^{N_B} e^{j2\theta_n}|f_{k,b}|^2\right)$. Finally, the distribution of the received SINR becomes: $|\rho\hat{\mathbf{g}}_k\mathbf{\Omega}\mathbf{H}\mathbf{f}_k|^2/\sigma_{MM}^2 \sim \exp(\xi)$, where ξ is the exponential parameter and can be written as

$$\xi = \frac{\left\{\Upsilon_1 + \Upsilon_2 + \sigma_k^2\right\}^2}{2N_R^2\left(\sum_{n=1}^{N_R}\sum_{b=1}^{N_B} e^{j2\theta_n}|f_{k,b}|^2\right)^2}, \tag{16}$$

where $\Upsilon_1 = \bar{\rho}^2(1-\alpha^2)\sum_{i=1}^{K}\sum_{b=1}^{N_B}\left|f_{i,b}\right|^2$ and $\Upsilon_2 = \rho^2(1-\beta^2)\sum_{i=1,i\neq k}^{K}\sum_{b=1}^{N_B}\left|f_{i,b}\right|^2$. ∎

Since the PDF of the received SINR follows an exponential distribution, the distribution/scale parameter refers to the mean of the distribution. The distribution parameter will determine the spread of the PDF; the larger the distribution parameter the larger the spread, and vice versa. In other words, for a smaller distribution parameter, the PDF curve is skewed towards the extreme values. Thus, high and low values of SINR are equally probable. Conversely, for a larger distribution parameter, the PDF curve has more spread; hence, there is a concentration on medium values of SINR. This insight helps us tune the system parameters (RIS configuration, etc.) under given correlation strengths between outdated and instantaneous CSI to achieve better performance at low cost and complexity.

Further, using the SINR expression, we find the Shannon capacity of a RIS-assisted mmWave channel under outdated CSI, which will allow us to find the moment generating function (MGF) of the channel service process. The Shannon capacity at the k^{th} MS for time slot l becomes

$$c_k(l) = B\log_2(1+\gamma_k(l)), \tag{17}$$

where B is the allocated bandwidth. Next, we find the EC of the RIS-enabled mmWave channel for different network settings when the CSI is outdated.

V. Effective Capacity Analysis of RIS-enabled mmWave Channel

In this section, we perform the EC analysis of the RIS-assisted mmWave channel under outdated CSI. We investigate the impact of the degree of optimisim of packet scheduling on the EC when the CSI is known to be outdated. Moreover, we provide a closed-form expression for the achievable EC, which incorporates the correlation strength between the outdated and instantaneous CSI, SINR distribution parameter, and the degree of optimism of packet scheduling. This closed-form expression allows us to understand the tradeoff between different system parameters, and consequently, helps us tune them for improved system performance at a low channel estimation cost.

The EC is an analytical tool to find the maximum constant arrival rate that can be supported by the time-varying channel conditions while satisfying the statistical QoS guarantees imposed at the transmitter's queue. It is defined as the log moment generating function (MGF) of the cumulative channel service process [30]. The EC at the k^{th} MS given that the

BS operates under certain QoS constraints (in terms of delay bound) becomes

$$\Pi_k(\nu) = -\frac{\Lambda(-\nu)}{\nu} = -\lim_{t\to\infty}\frac{1}{\nu t}\log(\mathbb{E}[e^{-\nu\sum_{l=1}^{t}s(l)}]), \quad (18)$$

where $s(l)$ is the service process during time slot l ($S(t) = \sum_{l=1}^{t}s(l)$ is the cumulative service process) and ν is the QoS exponent. Further, we assume that t is reasonably large so that we can invoke the Central limit theorem to approximate the distribution of $S(t)$, which becomes Gaussian [31]. Therefore, (18) becomes the log MGF of a Gaussian random variable, which can be written as

$$\Pi_k(\nu) = -\frac{\Lambda(-\nu)}{\nu} = \mathbb{E}[s(l)] - \frac{\nu}{2}\,\mathrm{var}[s(l)], \quad (19)$$

where $\mathbb{E}[s(l)]$ and $\mathrm{var}[s(l)]$ are the mean and variance of the service process, respectively. Further to find the EC, we recall that the BS has outdated CSI and it is aware of the imperfect nature of the available CSI. Therefore, in this case, the BS schedules packets of variable size for transmission depending upon the available CSI. However, due to the outdated nature of CSI, the transmitted packets will be lost from time to time. The packet loss ratio critically depends on the correlation between the outdated CSI and the real CSI for the upcoming time slot as well as the corresponding strategy for packet scheduling. In this case, the BS needs to schedule packets more carefully as it is aware of the erroneous CSI. Let $\hat{\gamma}_k(l)$ be the outdated CSI of the upcoming time slot l, then the scheduling decision at the BS is a function of the outdated CSI, which becomes: $a(l) = B\log_2(1+\delta^2\hat{\gamma}_k(l))$, where δ^2 is the SINR margin. Moreover, when $\gamma_k(l) \geq \delta^2\hat{\gamma}_k(l)$, the resulting service process becomes equal to the scheduled packets ($s(l) = a(l)$).

Before moving further with the calculation of the EC, we need to find the success probability of $a(l)$ given the correlation between the outdated and the real CSI for time slot l. The authors in [32] find the conditional PDF of the SINR for time slot l, which can help us find the success probability of $a(l)$. The conditional probability can be calculated using the following expression: $P_{x/\hat{\gamma}_k} = \xi/\bar{\rho}^2 I_o\big(2\xi\rho\sqrt{x\hat{\gamma}_k}/\bar{\rho}^2\big)e^{-\xi(x+\rho^2\hat{\gamma}_k)/\bar{\rho}^2}$, where I_o is the modified Bessel function of the first order. Further, given $\hat{\gamma}_k$ and $a(l)$, the success probability of the service process $s(l)$ can be calculated as

$$\begin{aligned}\mathbb{P}[s(l)=a(l)] &= \int_{\delta^2\hat{\gamma}_k}^{\infty}\frac{\xi}{\bar{\rho}^2}I_o\left(\frac{2\xi\rho\sqrt{x\hat{\gamma}_k}}{\bar{\rho}^2}\right)e^{\frac{-\xi(x+\rho^2\hat{\gamma}_k)}{\bar{\rho}^2}}dx\\ &\overset{(a)}{=} \int_{\delta\sqrt{2\xi\hat{\gamma}_k}/\bar{\rho}}^{\infty} uI_o\left(\frac{u\rho\sqrt{2\xi\hat{\gamma}_k}}{\bar{\rho}}\right)e^{\frac{-\bar{\rho}u^2-2\xi\rho^2\hat{\gamma}_k}{2\bar{\rho}}}du\\ &\overset{(b)}{=} \int_{\delta u_{\hat{\gamma}_k}}^{\infty} uI_o(u.\rho.u_{\hat{\gamma}_k})e^{\frac{-u^2+(\rho u_{\hat{\gamma}_k})^2}{2}}du = Q(\rho u_{\hat{\gamma}_k},\delta u_{\hat{\gamma}_k}).\end{aligned} \quad (20)$$

In (20), for equalities (a) and (b), we substitute $u = \sqrt{2\xi x}/\bar{\rho}$ and $u_{\hat{\gamma}_k} = \sqrt{2\xi\hat{\gamma}_k}/\bar{\rho}$, respectively, and Q is the Marcum Q-function.

Given the success probability of the service process in hand, we now aim to find the EC, and for that we need to find mean and variance of $s(l)$. The mean of $s(l)$ can be calculated using the following expression.

$$\begin{aligned}\mathbb{E}[s(l)] &= B\int_0^{\infty}\log_2(1+\delta^2x)Q_1(\rho u_{\hat{\gamma}_k},\delta u_{\hat{\gamma}_k})f_X(x)dx\\ &\overset{(a)}{=} \frac{B\xi}{\ln_2}\int_0^{\infty}\ln(1+\delta^2x)Q_1(\rho u_{\hat{\gamma}_k},\delta u_{\hat{\gamma}_k})e^{-\xi x}dx.\end{aligned} \quad (21)$$

Equality (a) comes from the fact that X is the received SINR at the k^{th} MS and $f_X(x)$ is the PDF of $X \sim \exp(\xi)$, as given in Lemma 2. Because the expression in (21) has a Q function, deriving the closed-form expression for the mean is quite involved. Therefore, we find an upper bound for $Q(\rho u_{\hat{\gamma}_k},\delta u_{\hat{\gamma}_k})$, which is based on a geometric approach [33], and it comes out to be the following

$$\begin{cases} Q(\rho u_{\hat{\gamma}_k},\delta u_{\hat{\gamma}_k}) & \leq \sum_{i=0}^{\Xi-1}D_i e^{-\xi x\varpi_{1,i}} \qquad \rho<\delta \\ Q(\rho u_{\hat{\gamma}_k},\delta u_{\hat{\gamma}_k}) & \leq 1-\sum_{i=0}^{\Xi-1}D_i e^{-\xi x\varpi_{2,i}} \\ & \quad +\sum_{i=0}^{\Xi-1}D_i e^{-\xi x\varpi_{3,i}} \qquad \rho\geq\delta \end{cases} \quad (22)$$

where $D_i = (\vartheta_{i+1}-\vartheta_i)/\pi$ for $\vartheta \in [0,\pi]$, $\Xi \in \mathbb{N}$, $\varpi_{1,i} = (\sqrt{\delta^2-\rho^2\sin^2\vartheta_i} - \rho\cos\vartheta_i)/\bar{\rho}^2$, $\varpi_{2,i} = (-\sqrt{\delta^2-\rho^2\sin^2\vartheta_{i+1}} - \rho\cos\vartheta_{i+1})/\bar{\rho}^2$, and $\varpi_{3,i} = (\sqrt{\delta^2-\rho^2\sin^2\vartheta_{i+1}} - \rho\cos\vartheta_{i+1})/\bar{\rho}^2$. Given the upper bound on the corresponding Q function, the expression in (21) for the case of $\rho<\delta$ becomes

$$\mathbb{E}[s(l)] \leq \frac{B}{\ln_2}\sum_{i=0}^{\Xi-1}\int_0^{\infty}\xi D_i\ln(1+\delta^2x)e^{-\xi x(1+\varpi_{1,i})}dx. \quad (23)$$

Applying integration by parts and after some simplification steps, the final expression for the mean of the service process when $\rho<\delta$ can be written as

$$\mathbb{E}[s(l)] \leq \sum_{i=0}^{\Xi-1}\frac{BD_ie^v}{\ln_2(1+\varpi_{1,i})}\mathbb{E}_1[v]. \quad (24)$$

In (24), $v = \xi(1+\varpi_{1,i})/\delta^2$ and $\mathbb{E}_1[\cdot]$ is the exponential integral function. Similarly, one can also find the mean of the service process for $\rho\geq\delta$ by using the expression of the Q-function given in (22). Further, to find the variance of the service process, we have the following expression

$$\mathrm{var}[s(l)] = \mathbb{E}[s^2(l)] - \mathbb{E}[s(l)]^2, \quad (25)$$

where $\mathbb{E}[s^2(l)]$ is the second moment of $s(l)$. For the case of $\rho<\delta$, it can be found using the following

$$\begin{aligned}\mathbb{E}[s^2(l)] &\leq \sum_{i=0}^{\Xi-1}\frac{B^2\xi^2D_i}{\ln^2(2)}\int_o^{\infty}(\ln(1+\delta^2x))^2e^{-\xi x(1+\varpi_{1,i})}dx\\ &= \sum_{i=0}^{\Xi-1}\frac{B^2D_ie^v}{\ln^2(2)(1+\varpi_{1,i})}\left(\ln^2(v)+2\eta\ln(v)+\eta^2+\frac{\pi^2}{6}\right)\\ &\quad -\sum_{i=0}^{\Xi-1}\frac{2B^2D_i\xi e^v}{\ln^2(2)\delta^2}{}_3\mathbf{F}_3\Big([1,1,1],[2,2,2],-v\Big).\end{aligned} \quad (26)$$

In (26), ${}_3\mathbf{F}_3$ is the hyper-geometric function and η is the Euler constant. By substituting (26) and (24) in (25), we can find the variance of $s(l)$. Similarly, one can also find variance of $s(l)$

for $\rho \geq \delta$ by using the expression of Q-function given in (22). Further, the final expression for the EC at the k^{th} MS of the RIS-assisted MISO system when the BS only has outdated CSI of the upcoming time slot l can be calculated by substituting mean and variance of $s(l)$ in (19). It is worth noting that the corresponding EC is a function of δ, which refers to the degree of optimism at the BS for packet scheduling. In addition, the right expressions for mean and variance of the service process need to be chosen to find the EC, which critically depends upon the relationship between the SINR margin (δ) and the correlation between the outdated and instantaneous CSI of the upcoming time slot (ρ).

This analysis allows us to tune the packet scheduling at the BS to achieve better EC even when the RIS is not optimally configured (due to the outdated CSI). Moreover, it provides a tradeoff between the degree of optimism in packet scheduling and the outdatedness of the CSI, which helps us find the optimal number of packets (to be transmitted) as the CSI ages. Through this approach, a RIS-assisted mmWave system can achieve better performance (in terms of throughput and QoS) even without perfectly estimating the channels, which can significantly reduce the signaling overhead.

VI. Evaluation

We now verify the analytical findings by means of simulations. We first explore the general relationship of correlation strength, QoS constraints, and packet scheduling on the EC. We then use these insights to investigate the impact of mobility on the speed with which CSI becomes outdated, different mechanisms to cope with outdated CSI, as well as, their impact on the correlation between instantaneous and outdated CSI. In particular, we can consider narrow vs. wide antenna beams, which trade off antenna gain and speed with which the gain is reduced, as well as required CSI estimation (or beam training) frequency. This allows to optimize the RIS and protocol configuration to achieve the best overall EC.

A. Simulation Setup

We are primarily interested in the channel between RIS and the user as it determines the capacity and required beam training overhead. For simplicity, we assume a 128 x 128 RIS with half-wavelength element spacing to be at the center of a circle and the user to move around the circle, so that the path loss is constant. We assume beam training at the RIS is similar to conventional IEEE 802.11ad/ay systems with a codebook of beam patterns that are tested sequentially. Furthermore, we assume the elevation angle remains same while the azimuth angle changes as the MS moves along the circle. We take IEEE 802.11ad/ay beam training as reference to gather more insights on the training overhead and EC of the MS taking user movement into account. Assume the RIS has 128 beam patterns; then the time taken to configure the link via RIS is 5.3 milliseconds according to IEEE 802.11ay standard [34]. For the simulations, we generate different beam patterns with varying beam widths using the beam pattern design given in [35].

B. Simulation Results

Fig. 2 presents the EC versus the correlation strength between the instantaneous and outdated CSI given different QoS constraints imposed at the BS. We observe that the EC almost remains the same when the correlation strength is low (for $\rho \leq 0.25$), but it increases rapidly as the CSI becomes less outdated (for $\rho > 0.25$). This is due to the fact that as the correlation strength increases, the probability of a higher received SINR also increases, which ultimately provides a better EC. Moreover, when the correlation coefficient is high, the BS can opt for an optimistic approach and schedule more packets for transmission and that leads to a better EC. In contrast, for a smaller correlation coefficient, the BS schedules packets to be transmitted more pessimistically, which limits the EC. Further, we observe from Fig. 2 that a lower EC is achieved when the BS operates under stringent QoS constraints. The impact of the QoS constraints on the EC becomes significant when the correlation strength between the instantaneous and outdated CSI is high. This is due to the fact that with a higher correlation coefficient, the BS optimistically schedules the packet to be transmitted, and with relaxed QoS constraints, the transmission queue at the BS can process more packets, thus allowing a significantly better EC. Conversely, with stringent QoS constraints imposed, the probability of packet loss during transmission (due to the randomness of the wireless channel and the demand for higher QoS guarantees) will increase, which increases the packet retransmissions (depending upon the retransmission scheme at use), and that limits the number of unique packets being processed at the transmission queue, which ultimately leads to a lower EC.

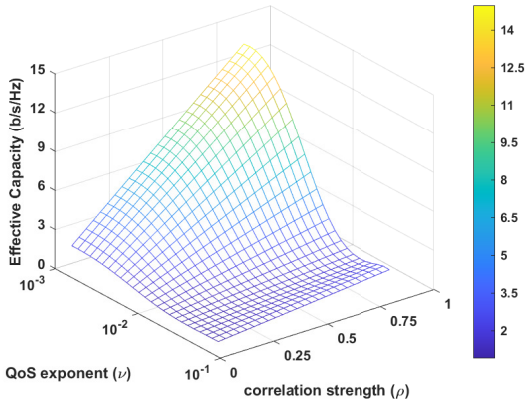

Fig. 2. Impact of correlation strength on the achievable effective capacity (EC) for different QoS constraints imposed at the BS.

Next, we provide a complete picture of the EC of the RIS-enabled mmWave link when the channel estimates are outdated. To this end, Fig. 3 presents a combined effect of different correlation strengths, SINR margins, and QoS exponents on the EC. We observe that there exists an optimal value of the SINR margin on which a maximum EC is achieved, and when the BS schedules the packets by following this optimal value,

the impact of outdatedness of the CSI becomes less significant. It leads us to believe that when the BS optimally schedules the packet, given the QoS constraints imposed at the transmission queue, the link provides better EC even with a lower correlation strength between outdated and instantaneous CSI. In other words, a conservative approach for RIS optimization, in which the RIS elements are configured less often, can also provide a better EC with less signaling overhead for channel estimation. This insight helps us apprehend the overall system design and provides the ground for a better understanding of the relation between the RIS configuration and the EC when the channel estimates are known to be outdated. It allows us to design different parameters of a RIS-assisted mmWave system in such a way that provides better performance (in terms of EC), while keeping the complexity and overhead at a minimum.

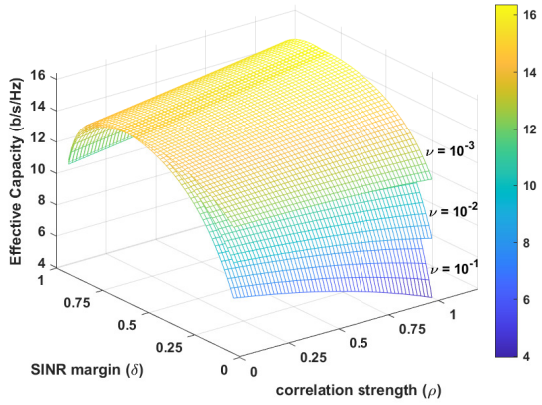

Fig. 3. Impact of the degree of optimism of packet scheduling at the BS on the achievable effective capacity (EC) for different QoS constraints imposed at the BS and different correlation strengths.

In Fig. 4, we investigate the impact of the correlation strength between the instantaneous and outdated CSI on the distribution parameter of the received SINR at the user. We observe that with perfect CSI (ρ = 1), RIS elements are optimally configured, which allows for a narrow beam directed towards the intended user. In this case, both high and low SINRs are equally probable because using a narrow beam can either provide coverage with full strength or it can miss the user entirely due to the fact that the CSI is outdated, and hence an outage occurs. In contrast, as the CSI becomes more outdated, one can use a conservative approach and not configure the RIS elements as often, which leads to a wider beam toward the user, and as a result, the probability of an outage reduces significantly because the probability that a wider beam misses the user entirely is lower. In this case, a high received SINR is less probable, but the user will have a medium SINR with high probability. This phenomenon is shown in Fig. 5, in which a comparison for aggressive and conservative RIS configuration approaches and their impact on the probability of received SINR is given. This tradeoff allows us to analyze the impact of the width of the beams given the network conditions and user mobility, i.e., how close to

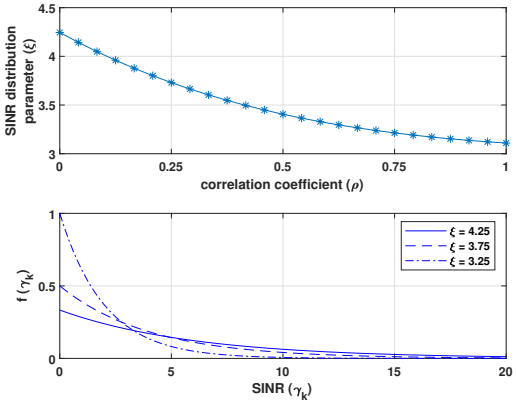

Fig. 4. Impact of correlation strength on the PDF and distribution parameter of the received SINR.

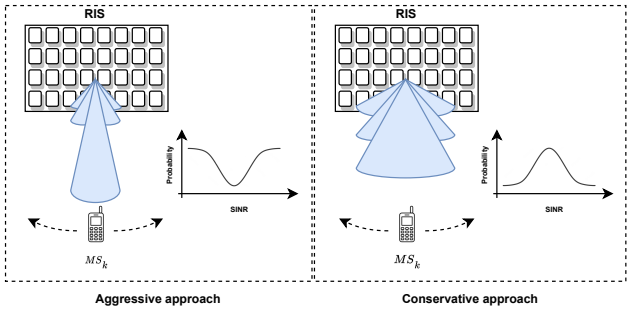

Fig. 5. Aggressive and conservative RIS configuration with outdated CSI.

optimal should the RIS elements be configured for the current CSI that is known to be outdated. To this end, we further investigate the impact of beam patterns on the EC by using varying beam widths.

Based on these findings, we now aim to find how often the RIS elements should be reconfigured, given a specific beam pattern in the context of outdated CSI to achieve better system performance. First, we investigate how the correlation strength between outdated and instantaneous CSI changes over time with MS mobility. We observe that for a narrow beam, the correlation strength quickly becomes weak as the user moves along the circumference of the RIS coverage (recall that MS distance from the RIS center remains the same). The correlation strength decreases more slowly for a wider beam for the same user velocity. Therefore, to achieve a certain threshold for a correlation strength, the RIS needs to be reconfigured more often for a narrow beam pattern and vice versa. To this end, Fig. 6 presents the impact of correlation strength on the EC for different beam patterns. We observe that the correlation strength for beam width = 5 degrees decreases rapidly over time (with MS velocity = 10 meter/s) compared to the correlation strength for beam width = 20 degrees. As the user moves along the circumference, it takes less time to move outside the beam coverage region for a narrower beam. Therefore, for a narrower beam to maintain a certain threshold

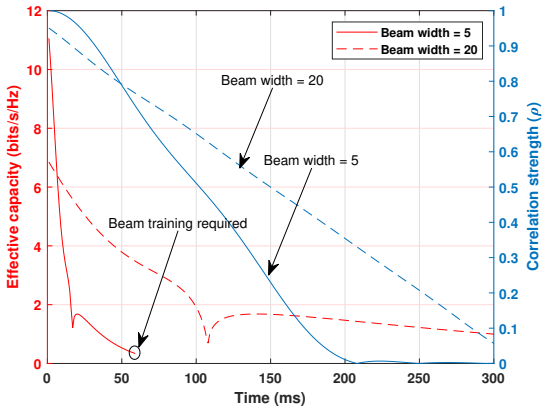

Fig. 6. Effective capacity (EC) and correlation strength over time with MS mobility = 10 meter/s for different beam patterns.

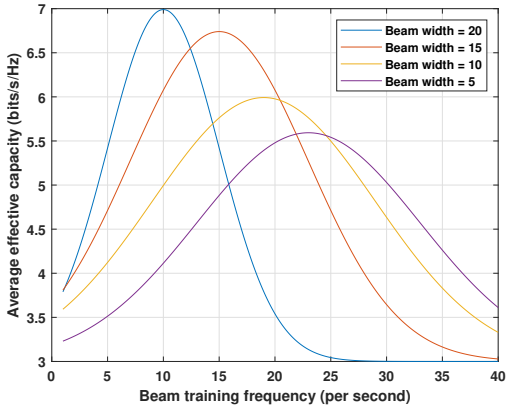

Fig. 7. Exhaustive search for an optimal beam training frequency for different beam widths.

for correlation strength, beam training should be done more often. For the EC, we also observe that it decreases over time rather quickly for a narrower beam (beam width = 5 degrees) compared to a wider beam (beam width = 20 degrees). This is because the correlation strength decreases more quickly for a narrower beam, which consequently reduces the EC. Another insight we get from here is that even though a higher EC can be achieved with a narrower beam, it degrades quickly with user mobility. In turn, beam training should be done more often to sustain better EC, which comes with the cost of extra signaling overhead. This highlights the importance of finding the optimal frequency for beam training given different beam patterns.

Fig. 7 presents an investigation to find the optimal beam training frequency for different beam patterns. Note that, to find the optimal value for beam training frequency, we subtract the time required for each beam training from the time allocated for data transmission; hence, there is less time for data transmission with a higher number of beam training procedures. We observe that as the frequency of the beam training increases, the average EC for all the beam patterns first increases, reaches an optimum, and then decreases. Therefore, there exists an optimal beam training frequency that provides the maximum average EC for a specific beam pattern. Moreover, we also observe that for a certain distance and MS velocity, as the beam becomes wider, a lower beam training frequency is required to achieve the maximum average EC (as shown in Fig. 6). Fewer beam trainings, in turn, result in more time for data transmission, which consequently increases the average EC. Further, we observe that a beam pattern with 20 degrees beam width can achieve significantly better EC with only 10 beam trainings per second when compared to a beam width of 5 degrees with 23 beam trainings per second. It shows that for a certain user velocity and distance from RIS, a wider beam can provide better performance at a much lower channel estimation cost.

VII. Conclusion

In this paper, we investigate the impact of outdated CSI on the effective capacity of a RIS-enabled mmWave network. Our analysis presents practical insights into the optimal design of the system parameters that provide good performance while keeping the complexity and cost associated with channel estimation to a bare minimum, given only the outdated channel estimates. Our simulation results reveal that the reflected beam pattern from the RIS has a direct impact on the correlation strength between outdated and instantaneous CSI. Moreover, our results demonstrate that a RIS needs to be reconfigured more often for a narrower beam pattern to maintain better effective capacity, which, in turn, increases the channel estimation cost. The results also show that an optimal beam training frequency exists for different beam patterns, which provides the maximum average effective capacity. Therefore, a suitable beam pattern, given the user's velocity and distance (from RIS), should be used, which not only provides better effective capacity but also keeps the signaling overhead associated with frequent channel estimation low. To further understand the optimal system design of a RIS-assisted mmWave network, we plan to investigate the impact of the distance between the RIS and the BS and the users (near and far-field scenarios) on the optimal selection of a beam pattern especially, when the system operates under outdated channel conditions. This analysis can provide insights into the RIS deployment strategy for mmWave networks in centralized and distributed RIS deployments.

Acknowledgment

This research work is sponsored by the European Union's Horizon 2020 research and innovation programme under Marie Sklodowska-Curie grant agreement no. 101061011 "RISE-MM", no. 861222 "MINTS", and the Spanish Ministry of Economic Affairs and Digital Transformation under European Union NextGeneration-EU projects TSI-063000-2021-59 RISC-6G and TSI-063000-2021-63 MAP-6G.

REFERENCES

[1] W. Jiang, B. Han, M. A. Habibi, and H. D. Schotten, "The road towards 6G: A comprehensive survey," *IEEE Open Journal of the Communications Society*, vol. 2, pp. 334–366, 2021.

[2] X. Wang, L. Kong, F. Kong, F. Qiu, M. Xia, S. Arnon, and G. Chen, "Millimeter wave communication: A comprehensive survey," *IEEE Communications Surveys & Tutorials*, vol. 20, no. 3, pp. 1616–1653, 2018.

[3] X. Tan, Z. Sun, D. Koutsonikolas, and J. M. Jornet, "Enabling indoor mobile millimeter-wave networks based on smart reflect-arrays," in *Proc. IEEE Conference on Computer Communications (IEEE INFOCOM)*, 2018, pp. 270–278.

[4] E. Basar, M. Di Renzo, J. De Rosny, M. Debbah, M.-S. Alouini, and R. Zhang, "Wireless communications through reconfigurable intelligent surfaces," *IEEE access*, vol. 7, pp. 116 753–116 773, 2019.

[5] M. Nemati, B. Maham, S. R. Pokhrel, and J. Choi, "Modeling RIS empowered outdoor-to-indoor communication in mmwave cellular networks," *IEEE Transactions on Communications*, vol. 69, no. 11, pp. 7837–7850, 2021.

[6] Y. Liu, X. Liu, X. Mu, T. Hou, J. Xu, M. Di Renzo, and N. Al-Dhahir, "Reconfigurable intelligent surfaces: Principles and opportunities," *IEEE communications surveys & tutorials*, vol. 23, no. 3, pp. 1546–1577, 2021.

[7] E. Basar, I. Yildirim, and F. Kilinc, "Indoor and outdoor physical channel modeling and efficient positioning for reconfigurable intelligent surfaces in mmwave bands," *IEEE Transactions on Communications*, vol. 69, no. 12, pp. 8600–8611, 2021.

[8] J. Zhang and D. M. Blough, "Optimizing coverage with intelligent surfaces for indoor mmWave networks," in *Proc. IEEE Conference on Computer Communications (IEEE INFOCOM)*, 2022, pp. 830–839.

[9] C. Feng, W. Shen, J. An, and L. Hanzo, "Joint hybrid and passive ris-assisted beamforming for mmwave mimo systems relying on dynamically configured subarrays," *IEEE Internet of Things Journal*, 2022.

[10] S. Ma, W. Shen, X. Gao, and J. An, "Robust channel estimation for RIS-aided millimeter-wave system with RIS blockage," *IEEE Transactions on Vehicular Technology*, vol. 71, no. 5, pp. 5621–5626, 2022.

[11] Y. Liu, S. Zhang, F. Gao, J. Tang, and O. A. Dobre, "Cascaded channel estimation for RIS assisted mmWave MIMO transmissions," *IEEE Wireless Communications Letters*, vol. 10, no. 9, pp. 2065–2069, 2021.

[12] T. Lin, X. Yu, Y. Zhu, and R. Schober, "Channel estimation for IRS-assisted millimeter-wave MIMO systems: Sparsity-inspired approaches," *IEEE Transactions on Communications*, vol. 70, no. 6, pp. 4078–4092, Jun. 2022.

[13] H. Zhang, B. Di, L. Song, and Z. Han, "Reconfigurable intelligent surfaces assisted communications with limited phase shifts: How many phase shifts are enough?" *IEEE Transactions on Vehicular Technology*, vol. 69, no. 4, pp. 4498–4502, 2020.

[14] D. Wu and R. Negi, "Effective capacity: a wireless link model for support of quality of service," *IEEE Transactions on wireless communications*, vol. 2, no. 4, pp. 630–643, 2003.

[15] N. S. Perović, M. Di Renzo, and M. F. Flanagan, "Channel capacity optimization using reconfigurable intelligent surfaces in indoor mmWave environments," in *Proc. 2020 IEEE International Conference on Communications (ICC 2020)*. IEEE, 2020, pp. 1–7.

[16] R. Li, S. Sun, and M. Tao, "Ergodic capacity maximization of RIS-assisted millimeter-wave MIMO-OFDM communication systems," *arXiv preprint arXiv:2205.13286*, 2022.

[17] S. W. H. Shah, A. N. Mian, S. Mumtaz, A. Al-Dulaimi, C.-L. I, and J. Crowcroft, "Statistical QoS analysis of reconfigurable intelligent surface-assisted D2D communication," *IEEE Transactions on Vehicular Technology*, vol. 71, no. 7, pp. 7343–7358, 2022.

[18] J. He, H. Wymeersch, and M. Juntti, "Channel estimation for RIS-aided mmWave MIMO systems via atomic norm minimization," *IEEE Transactions on Wireless Communications*, vol. 20, no. 9, pp. 5786–5797, 2021.

[19] G. Zhou, C. Pan, H. Ren, P. Popovski, and A. L. Swindlehurst, "Channel estimation for RIS-aided multiuser millimeter-wave systems," *IEEE Transactions on Signal Processing*, vol. 70, pp. 1478–1492, 2022.

[20] J. He, H. Wymeersch, M. Di Renzo, and M. Juntti, "Learning to estimate RIS-aided mmwave channels," *IEEE Wireless Communications Letters*, vol. 11, no. 4, pp. 841–845, 2022.

[21] F. Jiang, L. Yang, D. B. da Costa, and Q. Wu, "Channel estimation via direct calculation and deep learning for RIS-aided mmwave systems," *arXiv preprint arXiv:2008.04704*, 2020.

[22] E. Shtaiwi, H. Zhang, A. Abdelhadi, and Z. Han, "RIS-assisted mmwave channel estimation using convolutional neural networks," in *Proc. 2021 IEEE Wireless Communications and Networking Conference (IEEE WCNC) Workshops*. IEEE, 2021, pp. 1–6.

[23] C. You, B. Zheng, and R. Zhang, "Channel estimation and passive beamforming for intelligent reflecting surface: Discrete phase shift and progressive refinement," *IEEE Journal on Selected Areas in Communications*, vol. 38, no. 11, pp. 2604–2620, 2020.

[24] S. W. H. Shah, M. M. U. Rahman, A. N. Mian, O. A. Dobre, and J. Crowcroft, "Effective capacity analysis of HARQ-enabled D2D communication in multi-tier cellular networks," *IEEE Transactions on Vehicular Technology*, vol. 70, no. 9, pp. 9144–9159, 2021.

[25] H. Yang, Z. Xiong, J. Zhao, D. Niyato, L. Xiao, and Q. Wu, "Deep reinforcement learning-based intelligent reflecting surface for secure wireless communications," *IEEE Transactions on Wireless Communications*, vol. 20, no. 1, pp. 375–388, Jan. 2021.

[26] X. Guo, Y. Chen, and Y. Wang, "Learning-based robust and secure transmission for reconfigurable intelligent surface aided millimeter wave UAV communications," *IEEE Wireless Communications Letters*, vol. 10, no. 8, pp. 1795–1799, 2021.

[27] J. Xu and B. Ai, "When mmWave high-speed railway networks meet reconfigurable intelligent surface: a deep reinforcement learning method," *IEEE Wireless Communications Letters*, vol. 11, no. 3, pp. 533–537, 2021.

[28] Y. Zhang, J. Zhang, M. Di Renzo, H. Xiao, and B. Ai, "Reconfigurable intelligent surfaces with outdated channel state information: Centralized vs. distributed deployments," *IEEE Transactions on Communications*, vol. 70, no. 4, pp. 2742–2756, 2022.

[29] Q. Tao, J. Wang, and C. Zhong, "Performance analysis of intelligent reflecting surface aided communication systems," *IEEE Communications Letters*, vol. 24, no. 11, pp. 2464–2468, 2020.

[30] S. W. H. Shah, M. M. U. Rahman, A. N. Mian, A. Imran, S. Mumtaz, and O. A. Dobre, "On the impact of mode selection on effective capacity of device-to-device communication," *IEEE Wireless Communications Letters*, vol. 8, no. 3, pp. 945–948, 2019.

[31] B. Soret, M. C. Aguayo-Torres, and J. T. Entrambasaguas, "Capacity with explicit delay guarantees for generic sources over correlated Rayleigh channel," *IEEE Transactions on Wireless Communications*, vol. 9, no. 6, pp. 1901–1911, 2010.

[32] R. K. Mallik, "On multivariate Rayleigh and exponential distributions," *IEEE Transactions on Information Theory*, vol. 49, no. 6, pp. 1499–1515, 2003.

[33] N. Ding and H. Zhang, "A flexible method to approximate marcum Q-function based on geometric way of thinking," in *2008 3rd International Symposium on Communications, Control and Signal Processing*. IEEE, 2008, pp. 1351–1356.

[34] IEEE 802.11 working group, "Wireless LAN Medium Access Control (MAC) and Physical Layer (PHY) Specifications-Amendment 2: Enhanced Throughput for Operation in License-Exempt Bands Above 45 GHz," *IEEE Standard 802.11ay*, 2021.

[35] J. Palacios, D. De Donno, and J. Widmer, "Lightweight and effective sector beam pattern synthesis with uniform linear antenna arrays," *IEEE Antennas and Wireless Propagation Letters*, vol. 16, pp. 605–608, 2017.